ARTICLE OPEN

Check for updates

Pharmacological fingerprint of antipsychotic drugs at the serotonin 5-HT_{2A} receptor

Supriya A. Gaitonde[1], Charlotte Avet[1], Mario de la Fuente Revenga[2], Elodie Blondel-Tepaz[1], Aida Shahraki[3], Adrian Morales Pastor[4], Valerij Talagayev[3], Patricia Robledo[5], Peter Kolb[3], Jana Selent[4], Javier González-Maeso[2] and Michel Bouvier[1]✉

The intricate involvement of the serotonin 5-HT_{2A} receptor (5-HT_{2A}R) both in schizophrenia and in the activity of antipsychotic drugs is widely acknowledged. The currently marketed antipsychotic drugs, although effective in managing the symptoms of schizophrenia to a certain extent, are not without their repertoire of serious side effects. There is a need for better therapeutics to treat schizophrenia for which understanding the mechanism of action of the current antipsychotic drugs is imperative. With bioluminescence resonance energy transfer (BRET) assays, we trace the signaling signature of six antipsychotic drugs belonging to three generations at the 5-HT_{2A}R for the entire spectrum of signaling pathways activated by serotonin (5-HT). The antipsychotic drugs display previously unidentified pathway preference at the level of the individual Gα subunits and β-arrestins. In particular, risperidone, clozapine, olanzapine and haloperidol showed G protein-selective inverse agonist activity. In addition, G protein-selective partial agonism was found for aripiprazole and cariprazine. Pathway-specific apparent dissociation constants determined from functional analyses revealed distinct coupling-modulating capacities of the tested antipsychotics at the different 5-HT-activated pathways. Computational analyses of the pharmacological and structural fingerprints support a mechanistically based clustering that recapitulate the clinical classification (typical/first generation, atypical/second generation, third generation) of the antipsychotic drugs. The study provides a new framework to functionally classify antipsychotics that should represent a useful tool for the identification of better and safer neuropsychiatric drugs and allows formulating hypotheses on the links between specific signaling cascades and in the clinical outcomes of the existing drugs.

Molecular Psychiatry; https://doi.org/10.1038/s41380-024-02531-7

INTRODUCTION

Schizophrenia is a chronic, debilitating condition with an unknown etiology [1] affecting about 1% of the population worldwide. Antipsychotic drugs remain the mainstay of treatment, and are classified into typical (ex: haloperidol), atypical (ex: clozapine, olanzapine and risperidone) and third generation (ex: aripiprazole and cariprazine) based on their broad mechanism of action and side effect profile [2]. The higher affinity of atypical antipsychotics at the serotonin 5-HT_{2A} receptor (5-HT_{2A}R) compared to the dopamine D_2 receptor has been historically considered relevant for their lower tendency of causing extra pyramidal side effects (EPS) [3–5]. In addition, whereas activity at the dopamine D_2 receptor seems to be a prerequisite for effective antipsychotic activity, there is extensive evidence pointing towards the involvement of the 5-HT_{2A}R, not only in the mechanism of action of antipsychotics, but also in the pathophysiology of schizophrenia [6–9]. For instance, activation of the 5-HT_{2A}R by hallucinogenic compounds such as LSD is known to cause psychotic states similar to the positive symptoms of schizophrenia [10]. Moreover, studies over the years have detected changes in the expression levels of the 5-HT_{2A}R in patients with schizophrenia [9]; in fact the specific upregulation of the signaling via the 5-HT_{2A}R component of the 5-HT_{2A}R-$mGlu_2$R heterocomplex has been demonstrated to be an important contributing factor in schizophrenia symptoms [11–14]. Taking a step further, recent studies with postmortem samples of schizophrenia patients have identified functional selectivity at the G protein level for the 5-HT_{2A}R, with heightened signaling via the inhibitory $G\alpha_{i1}$ proteins versus the $G\alpha_q$ pathway [15].

The past two decades have seen an increasing appreciation of the therapeutic ramifications of functional selectivity across GPCRs with drug discovery efforts being directed towards teasing out the pathways leading to beneficial effects versus those causing side effects [16–24]. While the focus has been primarily between the G protein and β-arrestin pathways, bias among the different G protein subtypes is being uncovered as well [20, 25–27]. While current antipsychotic drugs such as clozapine, risperidone and olanzapine are known inverse agonists at the 5-HT_{2A}R [28, 29], little is known about their detailed functional selectivity profile at this critical receptor for schizophrenia treatment. A deeper

[1]Institute for Research in Immunology and Cancer (IRIC), Department of Biochemistry and Molecular Medicine, Université de Montréal, Montréal, QC H3T 1J4, Canada. [2]Department of Physiology and Biophysics, School of Medicine, Virginia Commonwealth University, Richmond, VA 23298, USA. [3]Department of Pharmaceutical Chemistry, Philipps-Universität Marburg, Marbacher Weg 8, 35032 Marburg, Germany. [4]Research Programme on Biomedical Informatics (GRIB), IMIM-Hospital del Mar Medical Research Institute, Barcelona 08003, Spain. [5]Integrative Pharmacology and Systems Neuroscience Research Group, IMIM-Hospital del Mar Medical Research Institute, Barcelona 08003, Spain. ✉email: michel.bouvier@umontreal.ca

Received: 12 May 2023 Revised: 6 March 2024 Accepted: 13 March 2024
Published online: 02 April 2024

understanding at the level of the different signaling pathways activated by serotonin (5-HT) could give an insight into their mechanisms of action and help shed some light on the pathophysiology of the disorder. Herein, with the suite of "Effector membrane translocation assay" (EMTA) enhanced bystander BRET (ebBRET) biosensors [20], we present the pharmacological fingerprint of six currently marketed antipsychotic drugs at the 5-HT_{2A}R with the aim of unveiling critical information on their mode of action and to set the stage for the development of safer, more efficacious antipsychotic drugs. The study also revealed characteristic signaling fingerprints corresponding to the three classes of antipsychotics and provides some insights into the pathways that may be underlying specific side effects.

MATERIALS AND METHODS

Reagents

Serotonin (5-HT), olanzapine and aripiprazole were purchased from Sigma-Aldrich, risperidone, clozapine and cariprazine were purchased from Cayman Chemical Company and haloperidol was purchased from Tocris bioscience. The $BRET^2$ substrates, coelenterazine 400a or DeepBlueC and [methoxy e-Coelenterazine (Me-O-e-CTZ)] or Prolume Purple were from Nanolight™ Technology.

Plasmids and cell culture

The human 5-HT_{2A}R was a gift from Domain Therapeutics North America. The human untagged G protein subunits were purchased from cdna.org. The following BRET-based biosensor components have been previously described: human G protein subunits, GRK2-D110A-GFP10, GRK2-GFP10, Gγ5-RlucII [30]; p63-RlucII [20], Rap1GAP-RlucII [20]; PDZ-RlucII [20]; $Gα_s$67-RlucII [31], β-arrestin1-RlucII, β-arrestin2-RlucII, rGFP-CAAX [25, 32].

All the experiments presented in this study were performed in HEK293 SL (hereafter named HEK293) clonal cell line, a gift from S. Laporte (McGill University, Montreal, Quebec, Canada), and have been described in [32], except in experiments comparing HEK293 cells backgrounds, where HEK293 T cells and the derived Bcm3 clonal cell line developed in Dr Bouvier's laboratory [33] were also used. Dulbecco's Modified Eagle Medium (DMEM), trypsin, newborn calf serum (NCS), fetal bovine serum (FBS), antibiotics [penicillin and streptomycin (PS)] and all other cell culture reagents were purchased from Wisent Inc. All cell lines were regularly tested for mycoplasma contamination.

Transfection

HEK293 cells were maintained in DMEM supplemented with 10% (v/v) NCS, 1% (v/v) antibiotics (100 U/mL penicillin and 100 µg/mL streptomycin; PS) and cultured in T150 cm^2 flasks (Corning®) at 37 °C with 5% CO_2 and 90% humidity. DNA mixtures (1000 ng adjusted with salmon sperm DNA; Invitrogen) were prepared in phosphate buffered saline (PBS; pH 7.4). Polyethyleneimine (PEI; Polysciences, Inc.) used for transfection was diluted in PBS, at a PEI:DNA ratio of 3:1, and was added to the DNA at least 15 min before addition of the DNA mix to the cells. A cell suspension of 3.5×10^5 cells/mL in DMEM was prepared and added to the DNA-PEI transfection mix, and immediately distributed (3.5×10^4 cells/100 µl/well) in 96-well white microplates (Greiner Bio-One) precoated with poly-L-ornithine (Sigma-Aldrich). The cells were maintained in culture for 48 h before conducting BRET experiments, except for the test evaluating whether 5-HT in the serum interfere with the activity of the receptor for which the cells were starved 24 h before BRET assay in 2% NCS (instead of 10% NCS normally). To determine receptor expression levels, saturation radioligand binding experiments were performed using [^{3}H]MDL100907 as previously reported [34]. The amount of 5-HT_{2A}R transfected across the different biosensors tested was the same and the receptor level determined to be 1675 fmol/mg protein.

To determine the G protein-activation profile of 5-HT across an entire panel of wild-type Gα subunits with the GRK2 biosensor, cells were transfected with the receptor, the respective Gα subunits, $Gβ_1$, $Gγ_5$-RlucII and GRK2-D110-GFP10 or GRK2-GFP10. To detect activation of a G protein pathway, cells were transfected with the receptor, the Gα subunit, and rGFP-CAAX along with either p63-RlucII, Rap1GAP-RlucII, PDZ-RlucII or $Gα_s$67-RlucII, depending on the Gα family being tested. For activation of $Gα_s$, $Gβ_1$ and $Gγ_1$ were co-transfected along with $Gα_s$67-RlucII. For recruitment of the β-arrestins, cells were transfected with the receptor, β-arrestin1-RlucII or β-arrestin2-RlucII, GRK2 and rGFP-CAAX.

Bioluminescence resonance energy transfer (BRET) assays

On the day of the BRET experiments, the cell culture medium was removed, and the cells were washed twice with PBS and treated with Tyrode's buffer (140 mM NaCl, 2.7 mM KCl, 1 mM $CaCl_2$, 12 mM $NaHCO_3$, 5.6 mM D-glucose, 0.5 mM $MgCl_2$, 0.37 mM NaH_2PO_4, 25 mM HEPES [pH 7.4]) and incubated at 37 °C for at least 15 min. To validate absence of effect from potential 5-HT present in the standard serum, cells were starved the night before the BRET assay in DMEM medium containing 2% of NCS (instead of 10% for regular experiments).

For the GRK2 recruitment-based biosensor used to establish which G proteins are engaged by the 5-HT_{2A}R, cells were treated with a supramaximal concentration of 5-HT and the ligands, incubated for 10 min after which the substrate coelenterazine 400a (2.5 µM) was added and the cells were incubated for 5 min before reading the BRET signal on the Spark® multimode microplate reader (Tecan) (acceptor, 515 ± 20 nm; and donor, 400 ± 70 nm filters).

Antipsychotics were tested in their agonist mode (in the absence of 5-HT) and antagonist mode (in the presence of 5-HT at its EC_{80}) using the EMTA biosensor suite with the same wavelength as above. For the concentration response curves of 5-HT and the ligands, cells were stimulated with different concentrations of the ligands and incubated for 5 min after which the substrate Prolume Purple (1.3 µM) was added and incubated for an additional 6 min. BRET signal was measured on the Spark® multimode microplate reader (Tecan) (agonist mode). Cells were thereafter treated with a submaximal concentration of 5-HT (EC_{80} concentration at the respective pathways) and incubated for an additional 5 min after which a second BRET read (antagonist mode) was conducted. To assess the role of $Gα_{i/o}$ proteins in 5-HT-mediated responses, cells were pretreated with pertussis toxin (PTX;100 ng/mL, 18 h; List Biological Laboratories) before agonist stimulation.

Computational analyses

To do the principal component analysis (PCA), signal transduction data was arranged in a 2-dimensional array where each pathway and metric pair was placed in the columns and drugs were arranged in rows. Each metric, i.e. IC_{50} and % of inhibition were scaled between 0 and 1 to eliminate the impact of the difference in range between them. After that, each drug was projected into the first 2 principal components of the row vectors using the python module scikit-learn.decomposition.

Docking studies

Various known structures of the serotonin 5-HT_{2A}R, including 6A93, 6A94, 7VOE, 7VOD, 6WHA and 7RAN were prepared using the protein preparation menu of Molecular Operating Environment (MOE) software, which is an integrated software package for drug discovery [35]. 3D structures of the six ligands were downloaded as mol2 files from the ZINC15 database at pH 7.4 [36]. In order to increase the variety of available poses, docking runs were conducted with either DOCK [37] or with HYBRID [38], which is included in the OEDocking suite (OEDOCKING 4.1.2.1: OpenEye Scientific Software, Inc., Santa Fe, NM. http://www.eyesopen.com). For docking calculations in HYBRID, receptors were prepared with pdb2receptor. Inputs for DOCK, which include receptor version with polar hydrogens, without hydrogens and a co-crystallized ligand in pdb format were prepared in MOE. Poses were visually selected for plausibility of binding mode (i.e. satisfaction of polar contacts, lack of intramolecular strain, absence of clashes with the receptor, etc). For consistency, the obtained poses were then subjected to energy minimization using the MMFF94x force field, which is a variant of MMFF94 (Merck Molecular force field) and is suitable for minimizing protein-ligand complexes [39] in MOE. During analysis, special attention was paid to the interaction with D3.32, as this residue is highly conserved among aminergic receptors. Risperidone in 6A93, aripiprazole in 7VOE and cariprazine in 7VOE were also minimized using the same force field. PyMOL (The PyMOL Molecular Graphics System, Version 2.0, Schrödinger, LLC) was used for visualization of the poses.

Animals and drugs

C57BL/6 wild-type males, sourced from JAX farms, 11 weeks of age at the time of experiment, were housed in groups of up to five littermates with food and water *ad libitum* in a vivarium with a 12 h light/dark cycle at 23 °C. Animals were allowed to get accustomed to the vivarium at least 1 week prior to the experiment. Experiments were conducted in accordance with NIH guidelines and were approved by the Virginia Commonwealth

University Animal Care and Use Committee. All efforts were made to minimize animal suffering and the number of animals used.

Risperidone and aripiprazole were sourced from Tocris bioscience. Risperidone was dissolved in saline 0.9% solution and aripiprazole in 10% DMSO-0.9% saline solution and administered intra-peritoneally (10 µL/g animal weight). The hydrochloride salts of risperidone and aripiprazole were formed in situ by addition of 1 eq. HCl. Aripiprazole was administered as a fine suspension.

IP1 experiment

Animals (5 animals per group) were sacrificed by cervical dislocation 1 h after drug (risperidone 3 mg/Kg and aripiprazole 2 mg/Kg) or vehicle and processed as previously described [40]. Briefly, frontal cortices were harvested and homogenized in a 10 µL per 1 mg of tissue solution consisting of 10% IP-One Gq Kit Lysis and Detection Buffer in Stimulation Buffer. The clarified homogenates (17,000 × *g* for 15 min) were plated in duplicate by sequential addition of 2 µL to a 18 µL mix of detection reagents in Lysis and Detection Buffer. The plates (HTRF 96-well low volume white plate, Cisbio-PerkinElmer) were read (emission at 615 and 665 nm following excitation at 320 nm and a 70 µs delay) within min of mixing at rt in a VICTOR Nivo (PerkinElmer) plate reader. The ratio between emission at 615 nm/665 nm for all conditions was calculated relative to the vehicle condition to determine the fold-change in IP1 concentration in the original sample. Standards ranging from 0 to 1.1 µM IP1 were employed to ensure linearity in the working concentrations used.

Data and statistical analyses

For in vitro experiments, curves fitting was conducted using GraphPad Prism 9 (version 9.0.0). Concentration response curves were obtained using a three-parameter logistic nonlinear regression model and the results are expressed as mean ± SEM of at least three independent experiments. Raw BRET data is defined as the ratio of the light intensity emitted by the acceptor (515 nm) over the light intensity emitted by the donor (410 nm) (rGFP/RlucII). Ligand-promoted BRET (ΔBRET) was determined by subtracting the BRET ratio of the vehicle condition from the BRET ratio of the ligand-treated conditions. For the agonist and antagonist modes, the ligand-promoted BRET was normalized with respect to the maximal response of 5-HT (% response of 5-HT), and BRET promoted by 5-HT at its EC_{80} concentration (5-HT(EC_{80})), respectively, to get the logEC_{50} and E_{max} and the logIC_{50} values.

The Cheng-Prusoff equation as modified by the Cheng 2002 paper [41] was used to calculate the equilibrium dissociation constant:

$$K_B = \frac{IC_{50}}{1 + \left[\frac{A}{EC_{50}}\right]^K}$$

where, IC_{50}: is the concentration of the compounds producing 50% of the inhibition of the activation mediated by the EC_{80} concentration (A) of 5-HT. *K* is the slope of the inhibition curve of the compounds tested in the antagonist mode. EC_{50} is the concentration of 5-HT producing 50% of the maximal response.

For in vivo experiments, no specific statistical method was used to calculate sample size, which was based on previous experiences with the same assays and are in line with the state of the art for similar assays. The mice used in the studies came from the same colony and were split randomly between the experimental groups. The investigators were blinded to group allocation during compounds administration to mice. Data are presented as mean ± SEM of 5 mice for each treated group.

Statistical significance was assessed with GraphPad Prism 9 (version 9.0.0) by Student's t-test (two-tailed) and ANOVA followed by Dunnett's post hoc test for multiple comparisons, performed as appropriate (see figure legends). The level of significance was chosen at $p < 0.05$.

RESULTS

Signaling profile of 5-HT at the 5-HT_{2A}R

As a first step in this study, we examined the complete G protein-activation profile of 5-HT at the predominantly $G\alpha_q$-coupled 5-HT_{2A}R in human embryonic kidney (HEK) 293 cells using a $BRET^2$ biosensor to rapidly determine the G protein subtypes engaged by a receptor-ligand pair. This biosensor, as previously described [30, 42], allows screening for the activation of an entire panel of wild-type Gα subunits belonging to the different families; $G\alpha_q$ (G_q, G_{11}, G_{14}, G_{15}), $G\alpha_{i/o/z}$ (G_{i1}, G_{i2}, G_{i3}, G_{oA}, G_{oB}, G_z), $G\alpha_{12/13}$ (G_{12}, G_{13}) and $G\alpha_s$. The assay is based on the detection of BRET between a GRK2 construct fused to the blue-shifted green fluorescent protein GFP10 (GRK2-GFP10) and $G\gamma_5$ fused to luciferase from *Renilla reniformis* (RlucII-$G\gamma_5$). The increase in BRET upon G protein-activation reflects the dissociation of Gα from Gγ thus allowing an association between the released RlucII-$G\gamma_5$ and GRK2-GFP10. We used a mutant form of GRK2 (D110A), which lacks the RGS domain for $G\alpha_q$, thus eliminating the possibility of a potential bias towards the detection of $G\alpha_q$ activation. Upon stimulation with 5-HT we observed robust activation of all members of the $G\alpha_q$ family ($G\alpha_q$, $G\alpha_{11}$, $G\alpha_{14}$, $G\alpha_{15}$) along with $G\alpha_z$ from the $G\alpha_{i/o/z}$ family (Fig. 1a). The results are comparable to those obtained using the wild-type (WT) form of GRK2-GFP10 (Supplementary Fig. 1a). Although this pattern of activation by 5-HT is in agreement with a recent study demonstrating the activation of mainly the $G\alpha_q$ family and $G\alpha_z$ with little or no activation of other $G\alpha_{i/o}$ family members [43], the 5-HT_{2A}R has also been reported to activate pathways downstream of the PTX-sensitive $G\alpha_{i/o}$ family, especially with respect to the pathophysiology of schizophrenia and the mechanism of action of hallucinogenic drugs [15, 20, 44, 45]. In particular, inverse agonist activity at $G\alpha_{i1}$ of the 5-HT_{2A}R-selective ligand (pimavanserin) was recently reported in human postmortem brain samples and mice brain cortices [26].

Hence, we further investigated the activation of the $G\alpha_{i/o/z}$ family using the more sensitive EMTA biosensors that measure the increase in BRET signal upon the recruitment of Gα family-specific effectors to the plasma membrane thus being a more direct reporter of the Gα activation state [20]. The assay used the Gα subunit selective effectors p63-RhoGEF for the $G\alpha_q$ family, PDZ-RhoGEF for $G\alpha_{12/13}$ and Rap1GAP for the $G\alpha_{i/o/z}$ family as well as $G\alpha_s$ itself fused to RlucII as the energy donor. The BRET between these donors and the *Renilla reniformis* GFP (rGFP) anchored at the inner face of the plasma membrane by the CAAX motif from Kras [20] is then used as an indicator of the G protein subtype activation. Similar to what was detected with the GRK2-based biosensor, we observed robust activation of the $G\alpha_q$ family members and $G\alpha_z$ (Fig. 1b, c). Moreover, we detected activation of the $G\alpha_{i/o}$ subtypes (Fig. 1c), and this response was found to be sensitive to pertussis toxin (PTX), suggesting direct activation of the different $G\alpha_{i/o}$ subunits by the 5-HT_{2A}R (Supplementary Fig. 1b). It is noteworthy that the activity detected in the absence of heterologous expression of Gα subunit was significantly reduced by PTX, reflecting the activation of endogenously expressed $G\alpha_{i/o}$. The remaining response observed in the presence of PTX most likely reflects activation of the endogenously expressed PTX- insensitive $G\alpha_z$, consistent with the robust response observed using either the GRK2- or Rap1GAP-based biosensors upon heterologous expression of $G\alpha_z$. Given that only weak coupling of 5-HT_{2A}R to $G\alpha_z$ *vs* other $G\alpha_{i/o}$ family members had been previously reported [43], we compared the residual $G\alpha_z$-mediated response following PTX treatment in three different HEK293 cell clones. As can be seen in Supplementary Fig. 1b, the PTX-resistant response represented between 40 ± 8 and 61 ± 7% of the global Rap1GAP response, indicating a cell type-dependent variation in the extent of $G\alpha_z$ coupling that may result from different relative expression of the $G\alpha_{i/o/z}$ subtypes in different clones. It should also be noted that Kim et al. used a BRET biosensor based on the dissociation between Gα and Gβγ subunits that, in contrast to the EMTA sensors used herein, requires modification of the Gα with the insertion of the energy donor Rluc in the Gα structure which may affect coupling and makes comparison between different Gα coupling difficult.

The activation of the $G\alpha_q$ and $G\alpha_{i/o/z}$ family observed in our study was entirely 5-HT_{2A}R-dependent since no responses were detected in the absence of 5-HT_{2A}R heterologous expression (Supplementary Fig. 1c). To exclude the possibility that 5-HT originating from the serum may interfere with the responses, experiments monitoring $G\alpha_q$ activation were carried out in cells

grown in media containing either 2% or 10% new calf serum (NCS). As shown in Supplementary Fig. 1d, no differences were observed, indicating that any possibly residual 5-HT did not interfere with the assay.

With the EMTA biosensor for $G\alpha_{12}$ and $G\alpha_{13}$ we confirm that the 5-HT_{2A}R does not directly activate $G\alpha_{12}$ or $G\alpha_{13}$ (Fig. 1d, e), in contrast to the robust activation observed for the TPα receptor used as a positive control. Although earlier studies have implicated $G\alpha_{12/13}$ in the activation of the phospholipase A_2 (PLA_2) pathway downstream of the 5-HT_{2A}R, other studies have also shown that there is no evidence for a direct coupling of these G proteins by the 5-HT_{2A}R [20, 43, 46]. No activation of $G\alpha_s$ (indicated by a decrease in BRET signal as a result of $G\alpha_s$67-RlucII leaving the plasma membrane decorated with the BRET acceptor rGFP as observed for 5-HT_{7A}R used as a positive control) was observed for the 5-HT_{2A}R upon 5-HT stimulation (Fig. 1f). In contrast to previously reported 5-HT-promoted cAMP accumulation in untransfected HEK293 cells [47], presumably due to the presence of endogenously expressed 5-HT_{7A}R, we did not detect any 5-HT-promoted activation of $G\alpha_s$ in untransfected cells (Supplementary Fig. 1e). This difference between the two studies may arise from different HEK293 clones being used or different sensitivities of the biosensors. In any case, no coupling of 5-HT_{2A}R to $G\alpha_s$ could be detected and this pathway was not further explored.

Activation of the 5-HT_{2A}R by 5-HT leads to the recruitment of the β-arrestins as seen with the robust signal observed with the EMTA biosensors (β-arrestin1 and β-arrestin2 respectively fused to RlucII recruited to the plasma membrane decorated with rGFP) (Fig. 1g, h). The potency of 5-HT ($logEC_{50}$ and $logEC_{80}$) for the activation of the different G protein subtypes and β-arrestin recruitment is presented in Supplementary Table 1.

Functional selectivity profile of antipsychotic drugs at the signaling pathways activated by 5-HT

Based on the signaling profile of 5-HT, we tested six antipsychotic drugs (risperidone, clozapine, olanzapine, aripiprazole, cariprazine and haloperidol) for their activity at the $G\alpha_q$ and $G\alpha_{i/o/z}$ family members and for the recruitment of the β-arrestins. When tested in the agonist mode, each antipsychotic has a specific activation/inactivation profile, providing a unique signaling signature, i.e., pathway-preference profile, of their activity at the 5-HT_{2A}R (Fig. 2). Our analyses reveal that the compounds can be divided into two groups, four having inverse agonist activity (risperidone, clozapine, olanzapine and haloperidol) and two being partial agonists (aripiprazole and cariprazine) on different pathways.

Risperidone, clozapine, olanzapine and haloperidol demonstrate pathway preference in their inverse agonist activity

Although antipsychotics have been reported to have inverse agonist activity at the 5-HT_{2A}R [29, 48], to our knowledge, this is

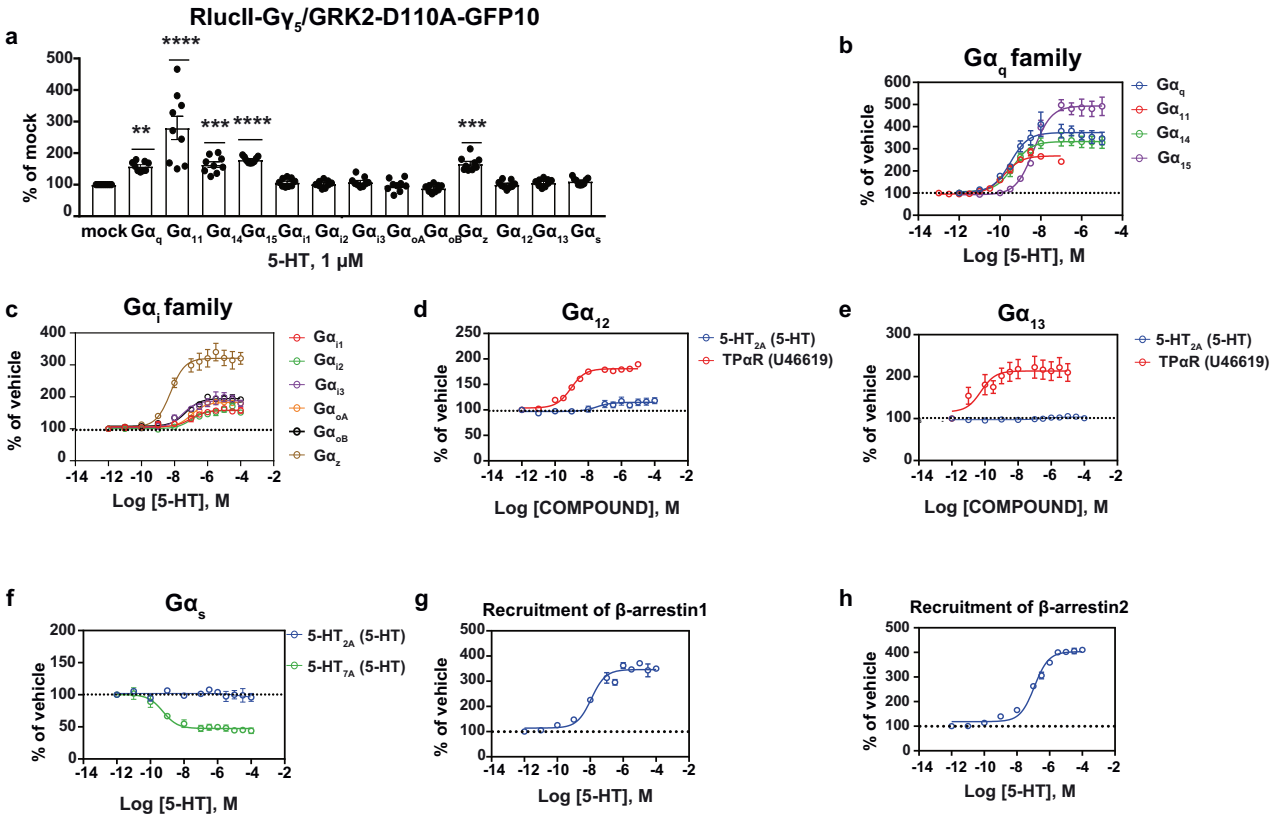

Fig. 1 The complete signaling profile of 5-HT at the 5-HT_{2A}R in HEK293 cells. a The complete G protein-activation profile of 5-HT (1 μM; 15 min) in HEK293 cells heterologously expressing the untagged 5-HT_{2A}R and the biosensor (RlucII-$G_{\gamma 5}$/GRK2-D110A-GFP10, $G\beta_1$ and the respective Gα subunits). Results are expressed as BRET ratio (GFP10/RlucII) as % of mock condition (in the absence of heterologously expressed Gα subunit) (mean ± SEM; $n = 3$; one-way ANOVA followed by Dunnett's post hoc: $^{**}p = 0.0029$, $^{***}p = 0.0009$, and $^{****}p < 0.0001$ compared to the mock condition). Concentration response curves showing the activation of the $G\alpha_q$ family (**b**), $G\alpha_{i/o/z}$ family (**c**), $G\alpha_{12}$ (**d**), $G\alpha_{13}$ (**e**), $G\alpha_s$ (**f**), as well as the recruitment of β-arrestin1 (**g**) or β-arrestin2 (**h**) using the ebBRET-based EMTA biosensor in HEK293 cells heterologously expressing the untagged 5-HT_{2A}R, the following biosensors (rGFP-CAAX along with p63-RlucII for $G\alpha_q$, Rap1GAP-RlucII for $G\alpha_{i/o/z}$, PDZ-RlucII for $G\alpha_{12}$ and $G\alpha_{13}$, $G\alpha_s$67-RlucII for $G\alpha_s$, β-arrestin1-RlucII or β-arrestin2-RlucII for β-arrestins), the respective Gα subunits ($G\alpha_q$ family, $G\alpha_{i/o/z}$ family, $G\alpha_{12/13}$), $G\beta_1$ and $G\gamma_1$ ($G\alpha_s$) or WT-GRK2 (β-arrestins). The HA-TPα receptor (U46619) was used as the positive control for $G\alpha_{12/13}$ while the 5-HT_{7A} receptor (5-HT) was used as the positive control for $G\alpha_s$. Results are expressed as BRET ratio (rGFP/RlucII), as % over vehicle (mean ± SEM; $n = 3$).

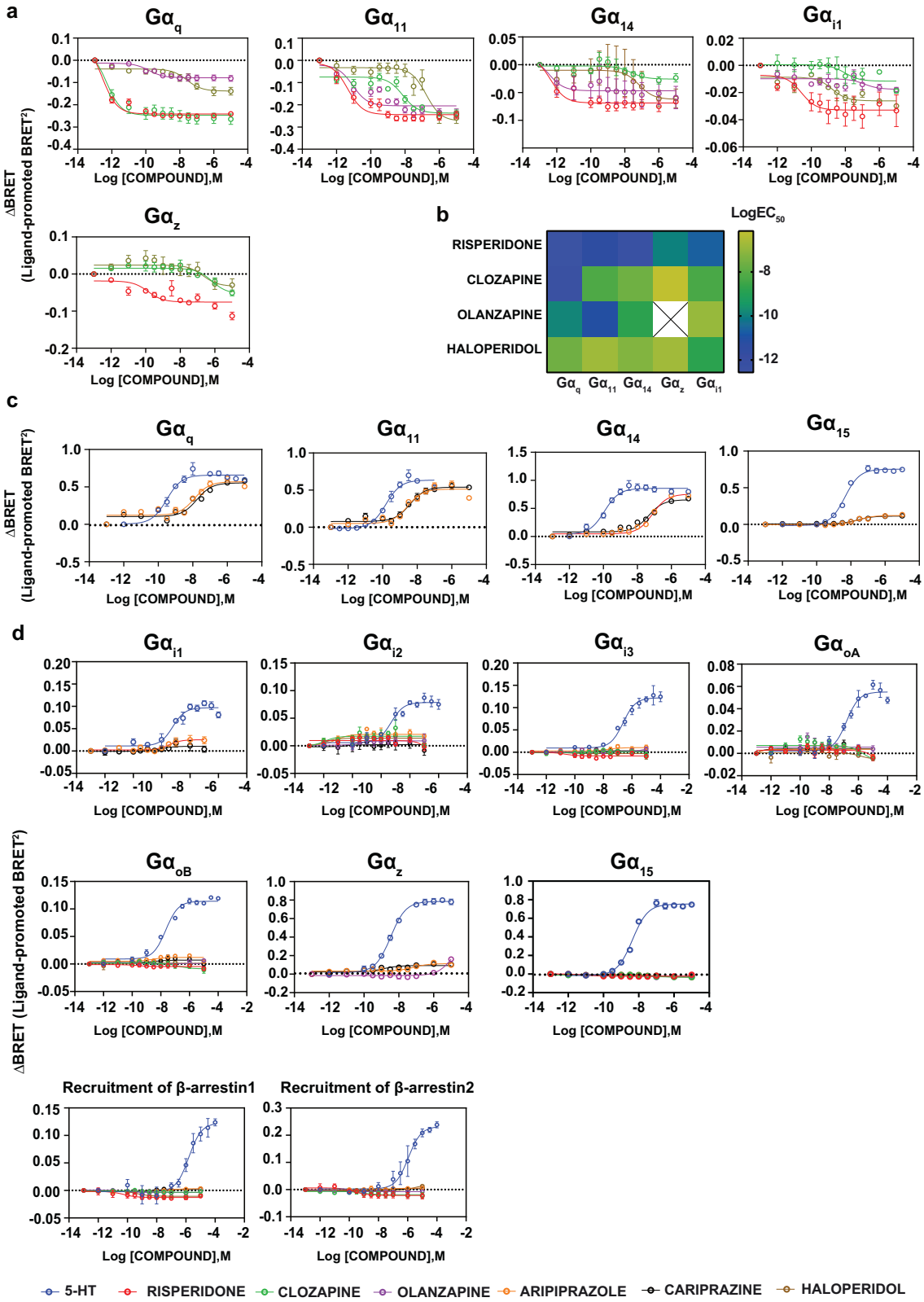

the first study assessing this activity for a set of antipsychotics at all the G protein subtypes engaged by this receptor. Overall, risperidone, clozapine, olanzapine and haloperidol were found to be inverse agonists (i.e.: inhibiting the constitutive activity of the 5-HT_{2A}R) mainly at $G\alpha_q$, $G\alpha_{11}$, $G\alpha_{14}$, $G\alpha_z$, and $G\alpha_{i1}$. No inverse agonist activity was detectable toward the other $G\alpha_{i/o}$ family members (G_{i2}, G_{i3}, G_{oA}, G_{oB}) or β-arrestin.

Among the four antipsychotics with inverse agonist activity, risperidone has the highest potency across different pathways (sub-picomolar and picomolar range at $G\alpha_q$, $G\alpha_{11}$ and $G\alpha_{14}$; Fig. 2b and

Fig. 2 Differential agonist and inverse agonist activities of the antipsychotic drugs at the G protein pathways and for recruitment of β-arrestins. a Concentration response curves depicting the inverse agonist activities of risperidone, clozapine, olanzapine and haloperidol using the ebBRET-based EMTA biosensors in HEK293 cells heterologously expressing the untagged 5-HT_{2A}R, the biosensor (rGFP-CAAX along with p63-RlucII for the $G\alpha_q$ family and Rap1GAP-RlucII for $G\alpha_{i1/z}$) and the respective Gα subunits. **b** Heatmap illustrating the potency ($logEC_{50}$) of inverse agonist activity shown by risperidone, clozapine, olanzapine and haloperidol from the concentration response curves. The empty cell with a cross indicates no inverse agonist activity. **c** Concentration response curves depicting the partial agonist activities of aripiprazole and cariprazine at the $G\alpha_q$ family using the ebBRET-based EMTA biosensors in HEK293 cells heterologously expressing the untagged 5-HT_{2A}R, the biosensor (rGFP-CAAX along with p63-RlucII for the $G\alpha_q$ family). **d** Curves of the six antipsychotic drugs at pathways where there was no activation when tested in the agonist mode using the ebBRET-based EMTA biosensors in HEK293 cells overexpressing the untagged 5-HT_{2A}R, the biosensors (rGFP-CAAX along with p63-RlucII for the $G\alpha_q$ family, Rap1GAP-RlucII for $G\alpha_{i/o/z}$ family, β-arrestin-RlucII/WT-GRK2 for β-arrestins) and the respective Gα subunits (for $G\alpha_q$ and $G\alpha_{i/o/z}$ families). Results are expressed as ΔBRET (ligand-promoted BRET) (mean ± SEM; $n = 3$).

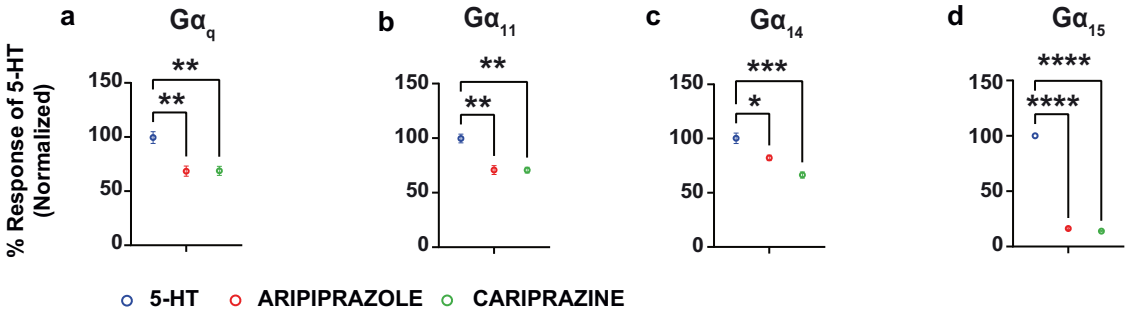

Fig. 3 Comparison of the activities of aripiprazole and cariprazine with 5-HT in the agonist mode. Graphs comparing the maximal response of aripiprazole and cariprazine with that of 5-HT at $G\alpha_q$ (**a**), $G\alpha_{11}$ (**b**), $G\alpha_{14}$ (**c**) and $G\alpha_{15}$ (**d**) (mean ± SEM; $n = 3$; one-way ANOVA followed by Dunnett's post hoc test). $^{**}p = 0.0046$ for aripiprazole and $^{**}p = 0.0047$ for cariprazine in **a**, $^{**}p = 0.0023$ in **b**, $^{*}p = 0.0169$, and $^{***}p = 0.0007$ for **c** and $^{****}p < 0.0001$ for **d**, compared to the maximal response by 5-HT at the respective pathways.

Supplementary Table 2). While risperidone showed comparable potency at the five pathways at which inverse agonism was observed, there were major differences in the inverse agonist potency of clozapine for the different G protein subtypes. It has the highest potency at $G\alpha_q$ (sub-picomolar; $logEC_{50}$: −12.31 ± 0.21) followed by $G\alpha_{i1}$ ($logEC_{50}$: −8.24 ± 0.70), $G\alpha_{11}$ ($logEC_{50}$: −8.16 ± 0.19), $G\alpha_{14}$ ($logEC_{50}$: −7.45 ± 0.30) and finally $G\alpha_z$ ($logEC_{50}$: −6.17 ± 0.29) (Fig. 2b and Supplementary Table 2). Of notice, the structurally-related antipsychotics clozapine and olanzapine differ significantly in their inverse agonist potency, which likely reflects the previously reported differences in the binding mode of these drugs with respect to the two serine residues in TM5 [49]. While the rank order of potency for clozapine is $G\alpha_q$ ($logEC_{50}$: -12.31 ± 0.21) ≫ $G\alpha_{i1}$ ($logEC_{50}$: −8.24 ± 0.70) = $G\alpha_{11}$ ($logEC_{50}$: −8.16 ± 0.19) > $G\alpha_{14}$ ($logEC_{50}$: −7.45 ± 0.30) > $G\alpha_z$ ($logEC_{50}$: −6.17 ± 0.29), it is $G\alpha_{11}$ ($logEC_{50}$: −11.06 ± 0.25) ≫ $G\alpha_q$ ($logEC_{50}$: −9.81 ± 0.22) > $G\alpha_{14}$ ($logEC_{50}$: −8.35 ± 0.34) ≫ $G\alpha_{i1}$ ($logEC_{50}$: −6.87 ± 0.81) ≫ $G\alpha_z$ (no activity) for olanzapine (Fig. 2b and Supplementary Table 2). Haloperidol, known primarily for its activity at the dopamine D_2 receptor, has the lowest overall potency among the four antipsychotics displaying inverse agonist activity at the 5-HT_{2A}R. It showed its highest potency at $G\alpha_{i1}$ ($logEC_{50}$: −8.77 ± 0.88) and no preference ($logEC_{50}$: −6.70 to −7.58) among the other four G proteins engaged ($G\alpha_q$, $G\alpha_{11}$, $G\alpha_{14}$ and $G\alpha_z$) (Fig. 2b and Supplementary Table 2).

Of interest, the relative inverse efficacy of the four compounds varied depending on the G protein subtype considered. Whereas haloperidol was the most efficacious compound for $G\alpha_{11}$ and $G\alpha_{14}$, the most efficacious one for $G\alpha_q$ was risperidone. The three compounds (risperidone, clozapine and haloperidol) with inverse agonist activity at $G\alpha_z$ were found to be equi-efficacious at this pathway (Supplementary Fig. 2). Taken together, the data unravel clear differences among clinically used antipsychotic to act as inverse agonists and displaying distinct G protein selectivity in their inverse potency and efficacy.

In addition to these compounds we also tested a clinically used antipsychotic for psychosis associated with Parkinson's disease, pimavanserin. As shown in Supplementary Fig. 3, similar to risperidone, clozapine, olanzapine and haloperidol (Fig. 2), pimavanserin showed a robust inverse agonist efficacy on $G\alpha_{q/11}$ family members. For the $G\alpha_{i/o/z}$ pathways, it showed a weak inverse efficacy for $G\alpha_{i1}$ but no other member of the $G\alpha_{i/o/z}$ family.

The partial agonist activity of aripiprazole and cariprazine

Aripiprazole and cariprazine display functional selectivity in their pattern of activation of the different G proteins. When considering the $G\alpha_{q/11}$ family members, the two compounds showed partial agonist activity with relatively high efficacies at $G\alpha_q$, $G\alpha_{11}$ and $G\alpha_{14}$ (their efficacies being between 67.74 ± 4.97 and 73.28 ± 3.61% of that of 5-HT) but only low efficacy partial agonists at $G\alpha_{15}$ (their efficacies being only 16.29 ± 0.71 and 13.93 ± 0.53% of that of 5-HT; Fig. 2c). The two compounds were found to have similar partial agonistic activity (potency and efficacy) at each of the $G\alpha_q$ family subtypes (Fig. 3 and Supplementary Table 3).

At $G\alpha_{i/o/z}$, very weak yet statistically significant activation was detected for aripiprazole only at $G\alpha_{i1}$ and $G\alpha_z$ (Supplementary Figs. 4 and 5). Cariprazine for its part did not show statistically significant activation at the $G\alpha_{i/o/z}$ family (Supplementary Figs. 4 and 5). Finally, aripiprazole showed very weak yet statistically significant recruitment of β-arrestin1 whereas cariprazine did not (Supplementary Figs. 4 and 5 and Supplementary Table 3). Together, the data show that the two compounds have a preferential partial agonistic activity at $G\alpha_q$ *vs* $G\alpha_i$. Differential agonistic activity was also observed toward members of the same Gα protein subtype, with $G\alpha_q$, $G\alpha_{11}$ and $G\alpha_{14}$ being preferred *vs* $G\alpha_{15}$ for the $G\alpha_{q/11}$ family and $G\alpha_{i1}$ and $G\alpha_z$ being preferred *vs* all other $G\alpha_{i/o/z}$ family members. This preference for specific G protein subtypes is reminiscent to the one observed for the 4 compounds that showed inverse agonistic activity (Fig. 2a), indicating that this selectivity is linked to the coupling preference of the receptor and not agonist-promoted pathway preferences of the ligands themselves. Yet the difference between inverse agonism and partial agonism at these G proteins between

risperidone, clozapine, olanzapine and haloperidol on the one hand and aripiprazole or cariprazine on the other clearly points to a difference in the ligand-promoted regulation of subsets of G protein subtypes between these two groups of antipsychotics.

To assess whether this difference in inverse agonism and partial agonism between antipsychotics could translate in in vivo settings, we measured the levels of D-myo-inositol 1 monophosphate (IP1) in the frontal pole of the cortical lobe dissected from mice treated with risperidone, or aripiprazole or the vehicle alone for 60 min. As shown in Supplementary Fig. 6, aripiprazole promoted a statistically significant 10.5 ± 1.6% increase in IP1 levels compared to the vehicle condition, consistent with the partial agonism toward $G\alpha_q$ that we observed in the cell-based assays. Risperidone treatment, for its part, led to a significant 9.2 ± 1.2% reduction in IP1 consistent with the inverse efficacy observed in cells. However, one cannot exclude the possibility that this decreases results from that antagonistic action of the drug inhibiting the activation resulting from endogenous 5-HT as ascertaining inverse agonism in vivo is always hampered by the possible tonic presence of endogenous agonists.

Activity of the antipsychotics tested in antagonist mode

We tested the antipsychotics for their effect on the 5-HT (EC_{80})-mediated activation of the different G protein pathways and on the recruitment of β-arrestins. As was observed in the agonist mode, the inverse agonist activity of risperidone, clozapine, olanzapine and haloperidol could be seen at $G\alpha_q$, $G\alpha_{11}$ and $G\alpha_{14}$ as reflected by the fact that the compounds not only fully antagonized the 5-HT-promoted BRET response but also promoted a BRET reduction below basal activity (Fig. 4a–c and Supplementary Table 4b). For $G\alpha_{15}$, $G\alpha_z$, $G\alpha_{i1}$, $G\alpha_{oB}$ and the β-arrestins, the four compounds behave as full antagonists and no inverse agonist activity could be detected (Fig. 4d-i and Supplementary Table 4b).

On account of being high efficacy partial agonists at $G\alpha_q$, $G\alpha_{11}$ and $G\alpha_{14}$, aripiprazole and cariprazine did not show antagonistic activity for the 5-HT (EC_{80})-mediated activation of these pathways (Fig. 3 and Supplementary Tables 3, 4a, b). In contrast, the two compounds were low potency full antagonists for $G\alpha_{oB}$, $G\alpha_z$ and β-arrestins, and in lieu of their weak partial agonist activity at $G\alpha_{15}$ and $G\alpha_{i1}$, they are partial antagonists with relatively high inhibitory efficacy at these pathways (inhibiting the 5-HT promoted responses by ~80% at $G\alpha_{i1}$; Figs. 3, 4 and Supplementary Table 4a, b). These data indicate that aripiprazole and cariprazine have pathway selective efficacies at the 5-HT_{2A}R.

Although not a direct indication of binding affinity, the IC_{50} values obtained at the different pathways were used to calculate the apparent equilibrium dissociation constants (K_b) of the antipsychotics (Fig. 4j) based on the modified Cheng-Prusoff equation [41]. Overall, the apparent affinities calculated from the functional data follow the order of measured affinities reported in the literature. However, the analyses reveal the existence of distinct functionally-derived apparent affinities for the different pathways considered, indicating that affinities derived from binding experiments cannot be used directly to predict how potent a drug will be at inhibiting a specific pathway. Good examples of this are provided by risperidone and olanzapine. Risperidone displayed a K_b 1000-times lower to inhibit $G\alpha_q$ than to block β-arrestin recruitment. For its part, the K_b of olanzapine to inhibit $G\alpha_q$ and inhibit the 5-HT-mediated β-arrestin recruitment were similar, but 100-fold lower than for inhibiting $G\alpha_{i1}$.

Figure 5 illustrates the overall antagonist and inverse agonist transducer engagement profiles observed for the six antipsychotic drugs. The web representation allows to clearly see that the drugs can be classified into three different clusters according to their relative efficacies and potencies toward the different G protein subtypes and β-arrestins. Risperidone, clozapine and olanzapine displayed what could be considered as a balanced profile since each of the drugs showed similar potencies and efficacies among the pathways. In sharp contrast, aripiprazole and cariprazine showed marked pathway preference, having antagonistic activity only at a subset of the pathways. Haloperidol fell into a category of its own, where pathway preference could be seen only when considering its potencies for the different pathways. Of significant notice, the three clusters correspond to the classification of these antipsychotics as defined by their therapeutic profiles, namely typical (haloperidol), atypical (risperidone, clozapine and olanzapine) and third generation (aripiprazole and cariprazine). This visual clustering based on their overall signaling profiles was further confirmed using principal component analysis of the data (Fig. 5b).

Given the clear separation into three groups at the pathway level, we were wondering whether this was also borne out at the structural level. To that end, we analyzed the existing experimental structural data for risperidone (6A93) [50], aripiprazole (7VOE) [51], and cariprazine (7VOD) [51] and generated docking-derived poses for the remaining three molecules. As can be seen in Fig. 5c, the poses of olanzapine and clozapine overlay well with the X-ray structure of the risperidone-bound receptor. Their three-ring (clozapine and olanzapine) and two-ring (risperidone) systems, respectively, are positioned deep in the pocket, close to Ser239, a residue that has been described as being involved in receptor activation networks [52]. The fact that in the poses of all three ligands hydrogen bond donors or acceptors are close to the side chain of Ser239 might point to a role of this residue in their similar pathway signatures (Fig. 5a). Aripiprazole and cariprazine are positioned even deeper along the z-axis, pointing into the space between helices 5 and 6. The binding modes of these two drugs are substantially overlapping, and the residues surrounding the deepest-binding portions are again made up of residues such as Phe332 (6.44) and V333 (6.45) implicated in receptor activation [52, 53], possibly leading to a distinct conformation which could be responsible for their partial agonism. We would like to note, however, that our docking calculations also yielded alternative poses for aripiprazole and cariprazine that bound more in the direction of the extracellular space. In these poses, the dihydroquinoline and urea motifs, respectively, are involved in higher numbers of polar contacts compared to the experimental structures (Supplementary Fig. 7). Still, even in these alternative poses, aripiprazole and cariprazine are highly congruent, providing a possible rationale for their similar signaling profiles. Finally, the pose of haloperidol is located somewhat in-between the other two regions, and lacks the bulky rings close to Ser239 that is a common motif for clozapine, olanzapine and risperidone. These analyses support the notion that the binding modes also cluster in 3 different groups in line with the signaling signature.

DISCUSSION

The exhaustive profiling of six clinically used antipsychotics belonging to the three classes of drugs allowed us to confirm some of the already known pharmacological properties of these compounds but also revealed an unprecedented level of functional selectivity, which could have therapeutic ramifications. The most salient differences include clear preferences of the compounds in terms of their efficacy for the different pathways engaged by the receptor.

When considering the inverse efficacy of the compounds, although previous studies have reported some level of inverse efficacy mainly at the $G\alpha_q$ pathway, our study reveals a much broader spectrum of inverse efficacies not only at $G\alpha_q$ but also at other G proteins, but not β-arrestins. In addition, different level of inverse agonistic activity both at the efficacy and potency levels were found between the different G proteins. For example, clozapine is a 10,000-fold more potent inverse agonist at $G\alpha_q$ compared to $G\alpha_{11}$, $G\alpha_{14}$, $G\alpha_z$ and $G\alpha_{i1}$, a characteristic that is not

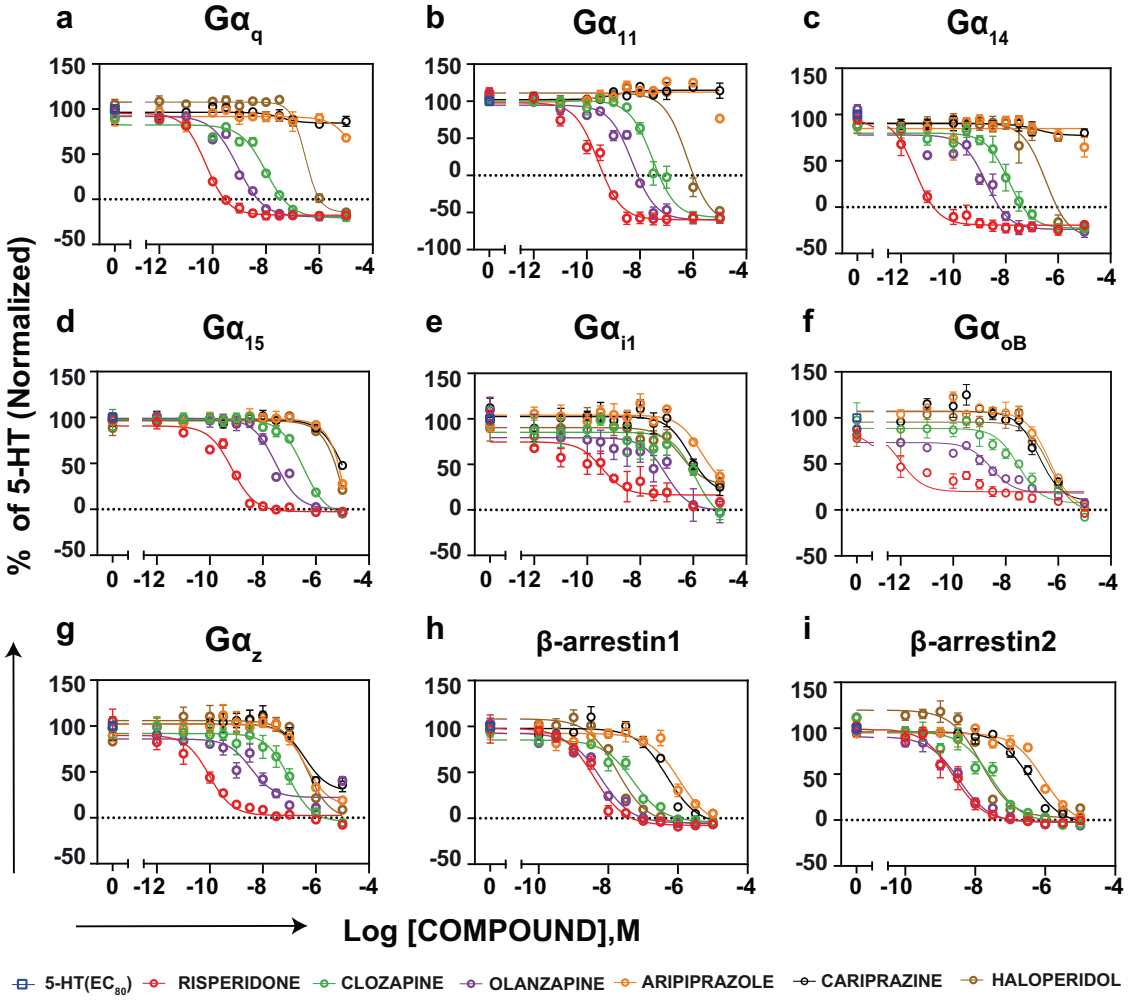

j

	RISPERIDONE	CLOZAPINE	OLANZAPINE	ARIPIPRAZOLE	CARIPRAZINE	HALOPERIDOL
Gq	-11.03	-8.76	-9.81	X	X	-7.17
G11	-10.45	-8.31	-9.11	X	X	-7.03
G14	-12.23	-8.53	-9.43	X	X	-7.19
G15	-10.03	-7.34	-8.38			
Gi1	-10.37	-6.60	-8.04	-6.51	-6.80	-7.13
GoB	-11.32	-7.99	-9.09	-6.87	-7.27	-6.82
Gz	-10.92	-7.73	-9.14	-7.05	-7.07	-7.00
ß-arrestin1	-9.17	-8.07	-8.96	-6.71	-7.07	-7.26
ß-arrestin2	-9.21	-8.15	-9.04	-6.62	-7.02	-7.20

ANTIPSYCHOTIC	Range of pK_i reported in the literature (radioligand binding)	REFERENCE
RISPERIDONE	8.27 – 10.0	a, b, c, d
CLOZAPINE	7.6 – 9.0	a, d
OLANZAPINE	8.6 – 8.9	a, b, d, e
ARIPIPRAZOLE	7.5 – 8.1	d, g
CARIPRAZINE	7.73	h
HALOPERIDOL	6.7 – 7.3	f

Fig. 4 Pathway-specific antagonistic activity of the six antipsychotic drugs tested. a-i Concentration response curves with the activity of the six antipsychotics tested in the antagonist mode (i.e; in the presence of an EC_{80} concentration of 5-HT) using the ebBRET-based EMTA biosensors in HEK293 cells heterologously expressing the untagged 5-HT_{2A}R and the biosensor (rGFP-CAAX along with p63-RlucII for $G\alpha_q$ family, Rap1GAP-RlucII for $G\alpha_{i/o/z}$, and the respective Gα subunits, as well as β-arrestin1-RlucII or β-arrestin2-RlucII and WT-GRK2 for recruitment of β-arrestins). Results are expressed as % response of 5-HT (EC_{80}) at the respective pathways (normalized with respect to the response of 5-HT (EC_{80})) (mean ± SEM; $n = 3–5$). **j** Heatmap depicting the equilibrium dissociation constant (K_b) of the antipsychotics calculated based on the modified Cheng-Prusoff equation as described in the methods section along with the pK_i values reported in the literature (**a** [66]; **b** [67]; **c** [68]; **d** [69]; **e** [70]; **f** [28]; **g** [56]; **h** [71]). The empty cells with a cross indicate no activity in the antagonist mode whereas cells colored blue indicate $IC_{50} > 10$ µM.

shared by the other antipsychotics with inverse efficacy. Whether this may have relevance for the distinct clinical therapeutic/side effect profile of clozapine remains to be investigated but it is worth noting that the inverse agonism of $G\alpha_q$ by clozapine through the 5-HT_{2A}R was found to potentiate $G\alpha_i$ signaling through the 5-HT_{2A}R-mGlu_2R heterocomplex that is upregulated in schizophrenia, and to be involved in the mechanism of its antipsychotic activity [12, 54].

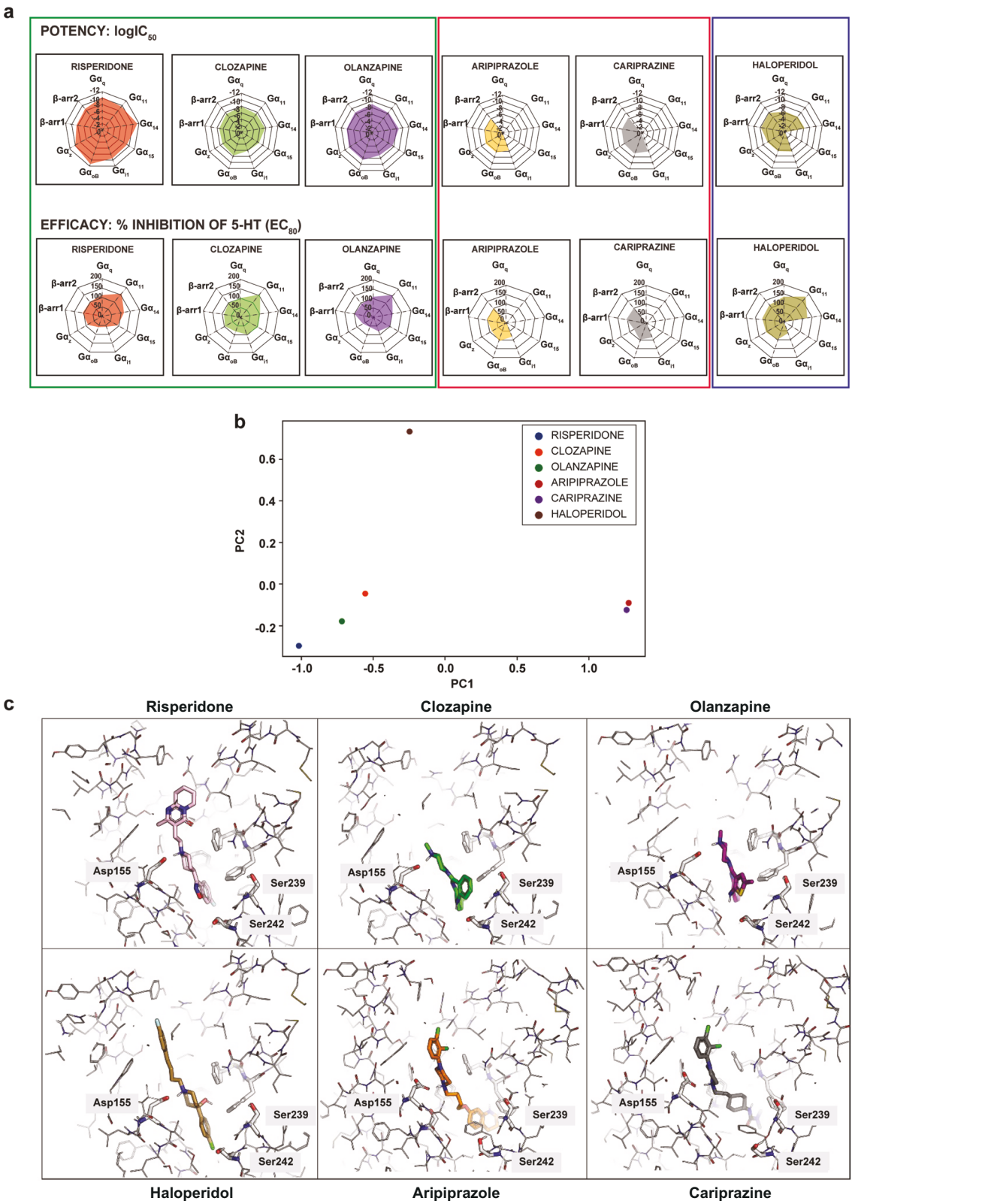

Fig. 5 Pharmacological and binding properties of the six antipsychotic drugs tested. a Web representation of the potency ($logIC_{50}$) and efficacy (% inhibition) of the six antipsychotics tested in the antagonist mode. **b** Principal component analysis of the antagonist mode (potency and efficacy) depicting the hierarchical clustering of the antipsychotics into three distinct groups. **c** Binding modes of the six antipsychotics at the 5-HT_{2A}R.

The only drug for which inverse efficacy at the 5-HT_{2A}R has previously been observed at a G protein other than $G\alpha_q$, namely $G\alpha_{i1}$, is the 5-HT_{2A}R-selective drug pimavanserin [26]. In the present study we found that four antipsychotics (risperidone, clozapine, olanzapine and haloperidol) are also inverse agonists at $G\alpha_{i1}$, whereas three of them (risperidone, clozapine and haloperidol) also showed inverse efficacy for one other member of the $G\alpha_{i/o/z}$ family, $G\alpha_z$. Previous studies have implicated $G\alpha_{i1}$ signaling through 5-HT_{2A}R activation in the mechanism of action of hallucinogenic drugs, and a supersensitive coupling of 5-HT_{2A}R to $G\alpha_{i1}$ as opposed to $G\alpha_q$ has been identified in the postmortem brain samples of schizophrenia patients. [7, 15, 26, 44].

Pimavanserin, which has been reported to be an inverse agonist at the 5-HT_{2A}R/$G\alpha_{i1}$ pathway [26] has been approved for Parkinson's disease-associated hallucinations and delusions. In the present study, pimavanserin, similar to risperidone, clozapine, olanzapine and haloperidol was found to be a robust inverse agonist on $G\alpha_{q/11}$ family members, whereas it showed only a weak inverse efficacy for $G\alpha_{i1}$ but not for other members of the $G\alpha_{i/o/z}$ family. Whether, as it was proposed for pimavanserin, the inverse agonism at $G\alpha_{i1}$ of risperidone, clozapine, olanzapine and haloperidol, measured in cell-based assays, may have the potential of being therapeutically useful in ameliorating the positive symptoms of schizophrenia remains to be investigated. The fact that pimavanserin, which was originally developed as an atypical antipsychotic is generally not used as a primary drug in schizophrenia patients [55] should also be considered in that context. Interestingly, the signaling profile obtained for pimavanserin is different from those observed for the six other antipsychotics tested.

Also, of interest is the selective high partial agonist efficacy of aripiprazole and cariprazine at $G\alpha_q$, $G\alpha_{11}$ and $G\alpha_{14}$ compared to their low efficacy partial agonist activity at $G\alpha_{15}$ and the mainly neutral antagonist activity at the $G\alpha_{i/o/z}$ family members and β-arrestins. Although previous studies have recognized these two D_2/D_3 and 5-HT_{1A} receptor-preferring antipsychotics for their antagonist activity at the 5-HT_{2A}R [56, 57], other studies have also detected partial agonist activity [51], thus underlying the fact that the cell type and pharmacological assay play a critical role, especially with regard to distinguishing partial agonism from neutral antagonism. The significant differences that we observe in the efficacy among the distinct G protein signaling pathways might be related to the inherent coupling efficiency of the 5-HT_{2A}R for the different G protein subtypes and the conformational state sampled by the ligand-bound receptor when coupled to different G proteins. The deviation of the activity at $G\alpha_{15}$ from the other members of the $G\alpha_q$ family most likely reflects the distinct characteristics of $G\alpha_{15}$ compared to the other members of the $G\alpha_{q/11}$ family [20, 58].

Although 5-HT_{2A}R agonists are associated with hallucinogenic properties and that aripiprazole and cariprazine are high efficacy partial agonists on some pathways ($G\alpha_q$, $G\alpha_{11}$ and $G\alpha_{14}$), the general absence of agonist efficacy at the $G\alpha_{i/o/z}$ family members could be one of the reasons why these compounds possess minimum risk of hallucinatory side effects. However, it would be pertinent to note here that the experimental system of the present study does not have heterologously expressed $mGlu_2R$, the heteromeric partner of the 5-HT_{2A}R shown to be contributing to the $G\alpha_i$ signaling through 5-HT_{2A}R in neurons [11].

In line with previous studies showing pharmacological and behavioral differences, especially between the typical antipsychotic haloperidol and the atypical drugs risperidone, clozapine and olanzapine [3, 59–65], our study unravels critical differences in the signaling profiles between antipsychotics belonging to the three different classes of clinically used antipsychotics. Remarkably, the pathway-specific equilibrium dissociation constants ($\log K_B$) highlight the differences in the capacity of the antipsychotics to engage the different signaling pathways. This illustrates the power of profiling the pathway preference and functional selectivity of compounds to classify drugs in different categories that may have clinical relevance and provide predictive value in drug discovery programs.

The distinct binding modes and docking poses of the six antipsychotic drugs along with the variations in the interactions with key amino acids in and around the binding pocket of the receptor is consistent with the fact that these compounds have different functional selectivity profiles. The similarities in the docking poses observed between antipsychotics belonging to a specific clinical category (atypical: risperidone, clozapine and olanzapine), (third generation: aripiprazole and cariprazine) that differed from haloperidol (typical) provides further insights in structural determinants of their distinct profiles both in clinical setting and signaling activities.

A limitation of the present study is that the signaling profile of the different antipsychotics at the 5-HT_{2A}R was carried out in HEK293 heterologously expressing the receptor and not in the neuronal cells which are the targets for these drugs. In addition to the cell type specificities, at 1675 fmol/mg protein, it is difficult to ascertain that the receptor expression level is within the physiological range as there is no reliable estimate of the receptor density at the synapse of the physiologically relevant nuclei. In any case, the results provide a useful profiling of the possible signaling repertoire of the 5-HT_{2A}R and of the distinct abilities of different antipsychotics to selectively regulate the signaling pathways of this repertoire. Validating the signaling profiles of the different antipsychotics in native tissues and test their impact on the therapeutic outcomes will await further in vivo experiments that will selectively be designed for this purpose. Yet, our observation that the partial agonisms of aripiprazole and inverse agonism of risperidone on the $G\alpha_q$ pathway could be confirmed by an elevation and decrease of IP1 levels, respectively, in the frontal cortical lobe of mice treated with these two drugs supports the possibility to translate our findings into physiological context.

A formal extrapolation of the functional selectivity profile of the antipsychotic drugs to their effect on specific symptoms of schizophrenia or side effects is beyond the scope of the present study. Yet the large data set generated in this simplified system have the distinct advantage of propounding functional selectivity at the level of individual G protein and β-arrestin pathways, and represent a stepping stone towards dissecting the signaling pathways associated with the therapeutic effects of antipsychotics from those leading to side effects.

DATA AVAILABILITY

All data needed to evaluate the conclusions in the paper are present in the paper and/or the Supplementary Materials.

MATERIALS AVAILABILITY

Some of the biosensors used in present study are protected by patents, but all are available for academic research under regular material transfer agreement (MTA) upon request to MB.

REFERENCES

1. Freedman R. Schizophrenia. N Engl J Med. 2003;349:1738–49.
2. Meltzer HY. Update on typical and atypical antipsychotic drugs. Annu Rev Med. 2013;64:393–406.
3. Meltzer HY, Matsubara S, Lee JC. Classification of typical and atypical antipsychotic drugs on the basis of dopamine D-1, D-2 and serotonin2 pKi values. J Pharmacol Exp Ther. 1989;251:238–46.
4. Schotte A, Janssen PF, Megens AA, Leysen JE. Occupancy of central neurotransmitter receptors by risperidone, clozapine and haloperidol, measured ex vivo by quantitative autoradiography. Brain Res. 1993;631:191–202.
5. Leysen JE, Janssen PM, Megens AA, Schotte A. Risperidone: a novel antipsychotic with balanced serotonin-dopamine antagonism, receptor occupancy profile, and pharmacologic activity. J Clin Psychiatry. 1994;55:5–12.

6. Meltzer HY, Huang M. In vivo actions of atypical antipsychotic drug on serotonergic and dopaminergic systems. Prog Brain Res. 2008;172:177–97.
7. Lopez-Gimenez JF, Gonzalez-Maeso J. Hallucinogens and serotonin 5-HT2A receptor-mediated signaling pathways. Curr Top Behav Neurosci. 2018;36:45–73.
8. Schmidt CJ, Sorensen SM, Kehne JH, Carr AA, Palfreyman MG. The role of 5-HT2A receptors in antipsychotic activity. Life Sci. 1995;56:2209–22.
9. Muguruza C, Moreno JL, Umali A, Callado LF, Meana JJ, Gonzalez-Maeso J. Dysregulated 5-HT(2A) receptor binding in postmortem frontal cortex of schizophrenic subjects. Eur Neuropsychopharmacol. 2013;23:852–64.
10. Nichols DE. Psychedelics. Pharmacol Rev. 2016;68:264–355.
11. Gonzalez-Maeso J, Ang RL, Yuen T, Chan P, Weisstaub NV, Lopez-Gimenez JF, et al. Identification of a serotonin/glutamate receptor complex implicated in psychosis. Nature. 2008;452:93–97.
12. Fribourg M, Moreno JL, Holloway T, Provasi D, Baki L, Mahajan R, et al. Decoding the signaling of a GPCR heteromeric complex reveals a unifying mechanism of action of antipsychotic drugs. Cell. 2011;147:1011–23.
13. Baki L, Fribourg M, Younkin J, Eltit JM, Moreno JL, Park G, et al. Cross-signaling in metabotropic glutamate 2 and serotonin 2A receptor heteromers in mammalian cells. Pflug Arch. 2016;468:775–93. https://doi.org/10.1007/s00424-015-1780-7
14. Moreno JL, Miranda-Azpiazu P, Garcia-Bea A, Younkin J, Cui M, Kozlenkov A, et al. Allosteric signaling through an mGlu2 and 5-HT2A heteromeric receptor complex and its potential contribution to schizophrenia. Sci Signal. 2016;9:ra5.
15. García-Bea A, Miranda-Azpiazu P, Muguruza C, Marmolejo-Martinez-Artesero S, Diez-Alarcia R, Gabilondo AM, et al. Serotonin 5-HT(2A) receptor expression and functionality in postmortem frontal cortex of subjects with schizophrenia: Selective biased agonism via G(αi1)-proteins. Eur Neuropsychopharmacol. 2019;29:1453–63.
16. Urban JD, Clarke WP, von Zastrow M, Nichols DE, Kobilka B, Weinstein H, et al. Functional selectivity and classical concepts of quantitative pharmacology. J Pharmacol Exp Ther. 2007;320:1–13.
17. Allen JA, Roth BL. Strategies to discover unexpected targets for drugs active at G protein-coupled receptors. Annu Rev Pharmacol Toxicol. 2011;51:117–44.
18. Tan L, Yan W, McCorvy JD, Cheng J. Biased ligands of G protein-coupled receptors (GPCRs): structure-functional selectivity relationships (SFSRs) and therapeutic potential. J Med Chem. 2018;61:9841–78.
19. Wingler LM, Lefkowitz RJ. Conformational basis of G protein-coupled receptor signaling versatility. Trends Cell Biol. 2020;30:736–47.
20. Avet C, Mancini A, Breton B, Le Gouill C, Hauser AS, Normand C, et al. Effector membrane translocation biosensors reveal G protein and βarrestin coupling profiles of 100 therapeutically relevant GPCRs. Elife. 2022;11:e74101.
21. Costa-Neto CM, Parreiras-E-Silva LT, Bouvier M. A pluridimensional view of biased agonism. Mol Pharmacol. 2016;90:587–95.
22. Galandrin S, Oligny-Longpre G, Bouvier M. The evasive nature of drug efficacy: implications for drug discovery. Trends Pharmacol Sci. 2007;28:423–30.
23. Stallaert W, Christopoulos A, Bouvier M. Ligand functional selectivity and quantitative pharmacology at G protein-coupled receptors. Expert Opin Drug Discov. 2011;6:811–25.
24. Fink EA, Xu J, Hübner H, Braz JM, Seemann P, Avet C, et al. Structure-based discovery of nonopioid analgesics acting through the α(2A)-adrenergic receptor. Science. 2022;377:eabn7065.
25. Namkung Y, LeGouill C, Kumar S, Cao Y, Teixeira LB, Lukasheva V, et al. Functional selectivity profiling of the angiotensin II type 1 receptor using pathway-wide BRET signaling sensors. Sci Signal. 2018;11:eaat1631.
26. Muneta-Arrate I, Diez-Alarcia R, Horrillo I, Meana JJ. Pimavanserin exhibits serotonin 5-HT(2A) receptor inverse agonism for G(αi1)- and neutral antagonism for G(αq/11)-proteins in human brain cortex. Eur Neuropsychopharmacol. 2020;36:83–89.
27. Wall MJ, Hill E, Huckstepp R, Barkan K, Deganutti G, Leuenberger M, et al. Selective activation of Gαob by an adenosine A(1) receptor agonist elicits analgesia without cardiorespiratory depression. Nat Commun. 2022;13:4150.
28. Egan CT, Herrick-Davis K, Teitler M. Creation of a constitutively activated state of the 5-hydroxytryptamine2A receptor by site-directed mutagenesis: inverse agonist activity of antipsychotic drugs. J Pharmacol Exp Ther. 1998;286:85–90.
29. Weiner DM, Burstein ES, Nash N, Croston GE, Currier EA, Vanover KE, et al. 5-hydroxytryptamine2A receptor inverse agonists as antipsychotics. J Pharmacol Exp Ther. 2001;299:268–76.
30. Mende F, Hundahl C, Plouffe B, Skov LJ, Sivertsen B, Madsen AN, et al. Translating biased signaling in the ghrelin receptor system into differential in vivo functions. Proc Natl Acad Sci USA. 2018;115:E10255–E10264.
31. Carr R 3rd, Du Y, Quoyer J, Panettieri RAJ, Janz JM, Bouvier M, et al. Development and characterization of pepducins as Gs-biased allosteric agonists. J Biol Chem. 2014;289:35668–84.
32. Namkung Y, Le Gouill C, Lukashova V, Kobayashi H, Hogue M, Khoury E, et al. Monitoring G protein-coupled receptor and β-arrestin trafficking in live cells using enhanced bystander BRET. Nat Commun. 2016;7:12178.
33. Schönegge A-M, Gallion J, Picard L-P, Wilkins AD, Le Gouill C, Audet M, et al. Evolutionary action and structural basis of the allosteric switch controlling β(2)AR functional selectivity. Nat Commun. 2017;8:2169.
34. Diez-Alarcia R, Muguruza C, Rivero G, García-Bea A, Gómez-Vallejo V, Callado LF, et al. Opposite alterations of 5-HT(2A) receptor brain density in subjects with schizophrenia: relevance of radiotracers pharmacological profile. Transl Psychiatry. 2021;11:302.
35. Molecular operating environment (MOE), 2013.08 Chemical Computing Group ULC, 910-1010 Sherbrooke St. W., Montreal, QC H3A 2R7, Canada, 2016.
36. Sterling T, Irwin JJ. ZINC 15–ligand discovery for everyone. J Chem Inf Model. 2015;55:2324–37.
37. Coleman RG, Carchia M, Sterling T, Irwin JJ, Shoichet BK. Ligand pose and orientational sampling in molecular docking. PLoS ONE. 2013;8:e75992.
38. McGann M. FRED and HYBRID docking performance on standardized datasets. J Comput Aided Mol Des. 2012;26:897–906.
39. Halgren TA. Merck molecular force field. I. Basis, form, scope, parameterization, and performance of MMFF94. J. Comput. Chem. 1996;17:490–519.
40. de la Fuente Revenga M, Shah UH, Nassehi N, Jaster AM, Hemanth P, Sierra S, et al. Psychedelic-like properties of quipazine and its structural analogues in mice. ACS Chem Neurosci. 2021;12:831–44.
41. Cheng HC. The power issue: determination of KB or Ki from IC50. A closer look at the Cheng-Prusoff equation, the Schild plot and related power equations. J Pharmacol Toxicol Methods. 2001;46:61–71.
42. Molinari P, Casella I, Costa T. Functional complementation of high-efficiency resonance energy transfer: a new tool for the study of protein binding interactions in living cells. Biochem J. 2008;409:251–61.
43. Kim K, Che T, Panova O, DiBerto JF, Lyu J, Krumm BE, et al. Structure of a hallucinogen-activated Gq-coupled 5-HT(2A) serotonin receptor. Cell. 2020;182:1574–88.e19.
44. Gonzalez-Maeso J, Weisstaub NV, Zhou M, Chan P, Ivic L, Ang R, et al. Hallucinogens recruit specific cortical 5-HT(2A) receptor-mediated signaling pathways to affect behavior. Neuron. 2007;53:439–52.
45. Inoue A, Raimondi F, Kadji FMN, Singh G, Kishi T, Uwamizu A, et al. Illuminating G-protein-coupling selectivity of GPCRs. Cell. 2019;177:1933–47.e25.
46. Kurrasch-Orbaugh DM, Parrish JC, Watts VJ, Nichols DE. A complex signaling cascade links the serotonin2A receptor to phospholipase A2 activation: the involvement of MAP kinases. J Neurochem. 2003;86:980–91.
47. Johnson MS, Lutz EM, Firbank S, Holland PJ, Mitchell R. Functional interactions between native Gs-coupled 5-HT receptors in HEK-293 cells and the heterologously expressed serotonin transporter. Cell Signal. 2003;15:803–11.
48. Sullivan LC, Clarke WP, Berg KA. Atypical antipsychotics and inverse agonism at 5-HT2 receptors. Curr Pharm Des. 2015;21:3732–8.
49. Selent J, Marti-Solano M, Rodriguez J, Atanes P, Brea J, Castro M, et al. Novel insights on the structural determinants of clozapine and olanzapine multi-target binding profiles. Eur J Med Chem. 2014;77:91–95.
50. Kimura KT, Asada H, Inoue A, Kadji FMN, Im D, Mori C, et al. Structures of the 5-HT2A receptor in complex with the antipsychotics risperidone and zotepine. Nat Struct Mol Biol. 2019;26:121–8.
51. Chen Z, Fan L, Wang H, Yu J, Lu D, Qi J, et al. Structure-based design of a novel third-generation antipsychotic drug lead with potential antidepressant properties. Nat Neurosci. 2022;25:39–49.
52. Hedderich JB, Persechino M, Becker K, Heydenreich FM, Gutermuth T, Bouvier M, et al. The pocketome of G-protein-coupled receptors reveals previously untargeted allosteric sites. Nat Commun. 2022;13:2567.
53. Hauser AS, Kooistra AJ, Munk C, Heydenreich FM, Veprintsev DB, Bouvier M, et al. GPCR activation mechanisms across classes and macro/microscales. Nat Struct Mol Biol. 2021;28:879–88.
54. Ibi D. Role of interaction of mGlu2 and 5-HT(2A) receptors in antipsychotic effects. Pharm Biochem Behav. 2022;221:173474.
55. Bugarski-Kirola D, Bitter I, Liu I-Y, Abbs B, Stankovic S. ENHANCE: Phase 3, randomized, double-blind, placebo-controlled study of adjunctive pimavanserin for schizophrenia in patients with an inadequate response to antipsychotic treatment. Schizophr Bull Open. 2022;3:sgac006.
56. Shapiro DA, Renock S, Arrington E, Chiodo LA, Liu L-X, Sibley DR, et al. Aripiprazole, a novel atypical antipsychotic drug with a unique and robust pharmacology. Neuropsychopharmacology. 2003;28:1400–11.
57. Herman A, El Mansari M, Adham N, Kiss B, Farkas B, Blier P. Involvement of 5-HT(1A) and 5-HT(2A) receptors but not α (2)-adrenoceptors in the acute electrophysiological effects of cariprazine in the rat brain in vivo. Mol Pharm. 2018;94:1363–70.
58. Giannone F, Malpeli G, Lisi V, Grasso S, Shukla P, Ramarli D, et al. The puzzling uniqueness of the heterotrimeric G15 protein and its potential beyond hematopoiesis. J Mol Endocrinol. 2010;44:259–69.
59. Ibi D, de la Fuente Revenga M, Kezunovic N, Muguruza C, Saunders JM, Gaitonde SA, et al. Antipsychotic-induced Hdac2 transcription via NF-kappaB leads to synaptic and cognitive side effects. Nat Neurosci. 2017;20:1247–59.

60. Willins DL, Berry SA, Alsayegh L, Backstrom JR, Sanders-Bush E, Friedman L, et al. Clozapine and other 5-hydroxytryptamine-2A receptor antagonists alter the subcellular distribution of 5-hydroxytryptamine-2A receptors in vitro and in vivo. Neuroscience. 1999;91:599–606.
61. Yadav PN, Kroeze WK, Farrell MS, Roth BL. Antagonist functional selectivity: 5-HT2A serotonin receptor antagonists differentially regulate 5-HT2A receptor protein level in vivo. J Pharmacol Exp Ther. 2011;339:99–105.
62. Tamminga CA. The science of antipsychotics: mechanistic insight. CNS Spectr. 2003;8:5–9.
63. Schrader JM, Irving CM, Octeau JC, Christian JA, Aballo TJ, Kareemo DJ, et al. The differential actions of clozapine and other antipsychotic drugs on the translocation of dopamine D2 receptors to the cell surface. J Biol Chem. 2019;294:5604–15.
64. Oranje B, Van Oel CJ, Gispen-De Wied CC, Verbaten MN, Kahn RS. Effects of typical and atypical antipsychotics on the prepulse inhibition of the startle reflex in patients with schizophrenia. J Clin Psychopharmacol. 2002;22:359–65.
65. Kumari V, Sharma T. Effects of typical and atypical antipsychotics on prepulse inhibition in schizophrenia: a critical evaluation of current evidence and directions for future research. Psychopharmacology. 2002;162:97–101.
66. Schotte A, Janssen PF, Gommeren W, Luyten WH, Van Gompel P, Lesage AS, et al. Risperidone compared with new and reference antipsychotic drugs: in vitro and in vivo receptor binding. Psychopharmacol (Berl). 1996;124:57–73.
67. Kongsamut S, Kang J, Chen X-L, Roehr J, Rampe D. A comparison of the receptor binding and HERG channel affinities for a series of antipsychotic drugs. Eur J Pharmacol. 2002;450:37–41.
68. Kroeze WK, Hufeisen SJ, Popadak BA, Renock SM, Steinberg S, Ernsberger P, et al. H1-histamine receptor affinity predicts short-term weight gain for typical and atypical antipsychotic drugs. Neuropsychopharmacology. 2003;28:519–26.
69. Younkin J, Gaitonde SA, Ellaithy A, Vekariya R, Baki L, Moreno JL, et al. Reformulating a pharmacophore for 5-HT2A serotonin receptor antagonists. ACS Chem Neurosci. 2016;7:1292–9.
70. Shahid M, Walker GB, Zorn SH, Wong EHF. Asenapine: a novel psychopharmacologic agent with a unique human receptor signature. J Psychopharmacol. 2009;23:65–73.
71. Kiss B, Horváth A, Némethy Z, Schmidt E, Laszlovszky I, Bugovics G, et al. Cariprazine (RGH-188), a dopamine D(3) receptor-preferring, D(3)/D(2) dopamine receptor antagonist-partial agonist antipsychotic candidate: in vitro and neurochemical profile. J Pharmacol Exp Ther. 2010;333:328–40.

ACKNOWLEDGEMENTS

We thank Monique Lagacé for critical reading of the manuscript, Christian Le Gouill for guidance during the project, Mireille Hogue for valuable scientific inputs, Christian Charbonneau for guidance with Adobe Illustrator, and Stefania Monteleone for providing an active-state model of the 5-HT_{2A}R.

AUTHOR CONTRIBUTIONS

SAG, PR, PK, JS and MB designed the study. SAG, CA, MdlFR, EB-T, AS and VT performed the experiments presented in this study. SAG, CA, EB-T. MdlFR, AMP, JG-M and MB participated in data analysis. SAG, CA, MdlFR, EB-T, AS, AMP, PR, PK, JS, JG-M and MB contributed to data interpretation. SAG, CA and MB prepared figures for publication. SAG and MB wrote the manuscript with input from all authors.

FUNDING

The work was funded by a Foundation Grant from the Canadian Institute for Health Research FDN148431 (MB), and a ERAnet NEURON consortium fund (funding was provided by CIHR NDD-161471 and FRQ-S 278647 for MB, the German Federal Ministry of Education and Research under grant number 01EW1909 for PK, as well as the Instituto de Salud Carlos III and Fondo Europeo de Desarrollo Regional number AC18/00030 for JS and PR). MB held a Canada Research Chair in Signal Transduction and Molecular Pharmacology. PK held a Heisenberg professorship KO4095/5-1 from the German Research Foundation DFG. PR acknowledges support from Instituto de Salud Carlos III grant PI18/00053 (Spain) and co-funding by the European Union. JG-M, held a National Institutes of Health NIH R01MH084894. EB-T received a bursary from a MITACS grant IT29484.

COMPETING INTERESTS

MB is the chair of the scientific advisory board of Domain Therapeutics, a biotech company to which some of the biosensors used in this study were licensed for commercial use. MdlFR is the owner of GONOGO solutions LLC. JG-M has as sponsor research contract with Terran Biosciences. None of the other authors declare competing interests.

ADDITIONAL INFORMATION

Supplementary information The online version contains supplementary material available at https://doi.org/10.1038/s41380-024-02531-7.

Correspondence and requests for materials should be addressed to Michel Bouvier.

Reprints and permission information is available at http://www.nature.com/reprints

Publisher's note Springer Nature remains neutral with regard to jurisdictional claims in published maps and institutional affiliations.